AIP Journal of Applied Physics

Crystalline ripples at the surface of ion eroded strained Si 0.8 Ge 0.2 epilayers

A. Kanjilal, S. Prucnal, M. Minniti, W. Skorupa, M. Helm, and S. Facsko

Citation: Journal of Applied Physics **107**, 073513 (2010); doi: 10.1063/1.3369391
View online: http://dx.doi.org/10.1063/1.3369391
View Table of Contents: http://scitation.aip.org/content/aip/journal/jap/107/7?ver=pdfcov
Published by the AIP Publishing

Articles you may be interested in
Origin of 90° domain wall pinning in Pb(Zr0.2Ti0.8)O3 heteroepitaxial thin films
Appl. Phys. Lett. **99**, 102902 (2011); 10.1063/1.3634028

Ion dose, energy, and species dependencies of strain relaxation of SiGe buffer layers fabricated by ion implantation technique
J. Appl. Phys. **107**, 103509 (2010); 10.1063/1.3374688

Strain relaxation in high Ge content SiGe layers deposited on Si
J. Appl. Phys. **107**, 063504 (2010); 10.1063/1.3327435

Fabrication of high-quality strain-relaxed thin SiGe layers on ion-implanted Si substrates
Appl. Phys. Lett. **85**, 2514 (2004); 10.1063/1.1794353

Detection of misfit dislocations at interface of strained Si/Si 0.8 Ge 0.2 by electron-beam-induced current technique
Appl. Phys. Lett. **84**, 3316 (2004); 10.1063/1.1734688

[This article is copyrighted as indicated in the article. Reuse of AIP content is subject to the terms at: http://scitation.aip.org/termsconditions. Downloaded to] IP: 142.104.240.194 On: Tue, 16 Dec 2014 15:53:14

Crystalline ripples at the surface of ion eroded strained $Si_{0.8}Ge_{0.2}$ epilayers

A. Kanjilal,[a] S. Prucnal, M. Minniti, W. Skorupa, M. Helm, and S. Facsko
Institute of Ion Beam Physics and Materials Research, Forschungszentrum Dresden-Rossendorf, P.O. Box 51 01 19, 01314 Dresden, Germany

(Received 28 January 2010; accepted 19 February 2010; published online 9 April 2010)

Surface erosion of a strained $Si_{0.8}Ge_{0.2}$ epilayer by 500 eV Ar^+ ions with a fluence of 4×10^{17} ions/cm^2 and the transformation from crystalline ripples to elongated Ge islands are reported by aligning the beam from 69° to 50° from the surface normal. Crystalline nature and the near surface Ge enrichment in such ripple structures are revealed by transmission electron microscopy. Moreover, ion beam induced decomposition of the SiGe network and the appearance of dislocation bands by suppressing the near-bandgap emission are manifested by μ-Raman and photoluminescence studies, respectively. © *2010 American Institute of Physics*.
[doi:10.1063/1.3369391]

I. INTRODUCTION

In the rapidly expanding world of nanotechnology patterning of solid surfaces, especially semiconductor surfaces with spatial periodicity in the tens of nanometer regime is now the subject of intense research because of their potential to fabricate photonic and magnetic devices. While traditional *top down* and *bottom up* approaches have generally been employed to fabricate ordered nanostructures, the development of self-assembled structures[1,2] such as ripples[1,3] and quantum dots[4,5] on semiconductor surfaces by means of an oblique ion erosion technique opens an inexpensive route to build functionalized substrates.[6,7] A large number of semiconductor[1–5] and metal[8] surfaces eroded by ion beam sputtering have been examined so far not only for developing functionalized substrates but also from a fundamental viewpoint (see recent review in Ref. 1). It is now well established that the competition between the surface roughening (due to the ion beam erosion) and smoothening (due to thermal or ion-induced material transport at the surface) mechanisms play a decisive role in forming periodic ripple patterns on amorphous/crystalline materials by ion beam erosion.[1] In a recent theoretical approach the formation of ripple patterns was also studied on alloy surfaces where the differences in sputter yields and surface diffusivities of the alloy components were predicted to lead the degree of alloy decomposition and spontaneous modulations in composition.[9]

In this context, silicon-germanium alloy surfaces would be ideal for understanding the formation of the compositionally modulated ripples through sputtering of the constituent elements, namely silicon (Si) and germanium (Ge). Although the reason behind the composition related differential sputtering yields of $Si_{1-x}Ge_x$ $(0 \leq x \leq 1)$ is still controversial, it has recently been suggested that the surface binding energy of an individual atom, atomic mass, atomic number and even atomic density are important to explain the observed nonlinear phenomena.[10,11] In fact, strain induced formation of *self-organized* nanostructure arrays has also been reported in epitaxially grown $Si_{1-x}Ge_x$ layers on (001)Si (see Ref. 12 for details). Using secondary ion mass spectrometry, Sarkar *et al.*[13] reported the nature of surface corrugation on strained, relaxed and polycrystalline SiGe layers when bombarded with 1 keV oxygen ions at an angle of 48° from the surface normal.

In this work, we present the morphological change at the surface of a strained $Si_{0.8}Ge_{0.2}$ epilayer by bombardment with Ar^+ ions at varying incidence angle (θ) and try to understand the impact on strain and ripple patterns, and the corresponding photoluminescence (PL) properties. In particular, we show the formation of crystalline SiGe rippled surfaces by aligning the ion beam to 69° from the surface normal. We also demonstrate that Si atoms are preferentially sputtered from the SiGe layers promoting Ge enrichment at the surface. Temperature dependent PL spectra show that the near-bandgap (NBG) emission from the $Si_{0.8}Ge_{0.2}$ layers completely disappears if the SiGe layer is further sputtered to the interface.

II. EXPERIMENTAL

By means of chemical vapor deposition technique, a 200 nm thick strained $Si_{0.8}Ge_{0.2}$ epilayer was grown at 650 °C on chemically cleaned *p*-type Si(100) wafers using silane (SiH_4) and germane (GeH_4) gas mixture with hydrogen as a carrier gas. Small pieces with area $\sim 1 \times 1$ cm^2 were cut from the wafer. The $Si_{0.8}Ge_{0.2}$ layers were then bombarded with a beam of 500 eV Ar^+ ions from a Kaufman type ion source with a fixed ion fluence of 4×10^{17} ions/cm^2 in a high vacuum chamber. The ion beam was aligned between 50°–70° from the surface normal to optimize θ for achieving ripple patterns. All sputtered samples were analyzed by atomic force microscopy (AFM). Depth profiles and incorporation of foreign metal atoms were examined by Rutherford backscattering spectrometry and energy dispersive x-ray spectroscopy (EDS). To determine the structure, cross-sectional transmission electron microscopy (XTEM) and aberration corrected high-angle-annular-dark-field (HAADF) scanning TEM (STEM) in combination with EDS were employed in an FEI TITAN 80–300 S/TEM instrument operating at 300 keV. The PL measurements were carried out at various temperatures in the range of 15–295 K by mounting the investigating sample in a closed-cycle helium cryostat,

[a]Electronic mail: a.kanjilal@fzd.de.

 © 2010 American Institute of Physics

[This article is copyrighted as indicated in the article. Reuse of AIP content is subject to the terms at: http://scitation.aip.org/termsconditions. Downloaded to] IP: 142.104.240.194 On: Tue, 16 Dec 2014 15:53:14

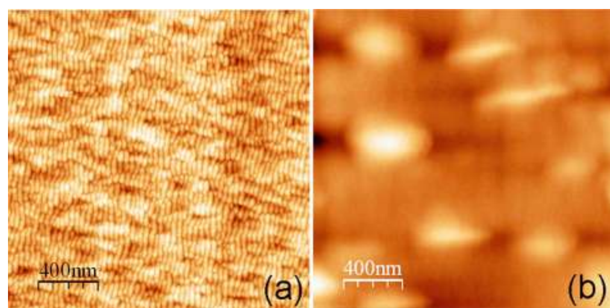

FIG. 1. (Color online) The AFM images of the 500 eV Ar^+ ion bombarded $Si_{0.8}Ge_{0.2}$ epilayer at an angle of (a) 69° and (b) 50° from the surface normal, showing ripple patterns and Ge islands on the surface, respectively.

while the samples were excited with the 532 nm line of a Nd:YAG (neodymium-doped yttrium aluminum garnet) laser with a power of 50 mW. Complementary results were obtained from 532 nm YAG laser (power on sample surface ~1 mW) excited μ-Raman spectra, recorded in the scattering geometry with a liquid nitrogen cooled charge-coupled device camera in a Raman microscope. The PL signals were analyzed with a single grating monochromator (TRIAX-550) and detected by an InGaAs detector in the infrared region with a standard lock-in technique where the laser beam was modulated at a frequency of 14 Hz by a rotating chopper.

III. RESULTS AND DISCUSSION

Figure 1 shows the surface topography of the samples sputtered at an incidence angle θ of 69° (a) and 50° (b), named as S69 and S50, respectively, signifying a strong influence of θ on surface morphology. In fact, only around an incidence angle of $65 \pm 5°$ the formation of pronounced self-organized ripple patterns was observed, similar to our findings for Si. At 69° ripple patterns with a period of ~40 nm and an average length of ~400 nm are formed on the SiGe layers [Fig. 1(a)], whereas self-assembled elongated Ge islands (confirmed by EDS measurements) were observed in S50 with a root-mean-square roughness of ~3 nm [Fig. 1(b)]. We checked the microstructure of S69 using XTEM and HAADF-STEM by keeping the electron beam close to the [011]-zone axis, showing crystalline ripples (Fig. 2), in contrary to the one commonly observed in ion eroded Si substrates.[1] A thin (~2 nm) amorphous layer was, however, noticed on top of such crystalline ripples. Moreover, close inspection reveals a dark contrast—called "Side-A," whereas "Side-B" does not have any variation in contrast [see Figs. 2(a) and 2(b)]. The corresponding high-resolution XTEM image [Fig. 2(c)] shows two distinct features near the surface: dislocations (zigzag lines) and missing atoms (marked by a box), while they are not regular in all ripples. The zone, which is marked by white dashed box [Fig. 2(c)] is magnified in Fig. 2(d) for clarity. One can also see the surface undulation with an average periodicity of ~40 nm in the HAADF-STEM image [Fig. 2(e)]. Please note that the HAADF-STEM intensity of an atom depends mainly on the atomic number Z, roughly $Z^{1.7}$ (Ref. 14). As the Z value of a Ge atom (32) is more than twice the one of Si (14), the contrast of a Ge atom will be about four times stronger than

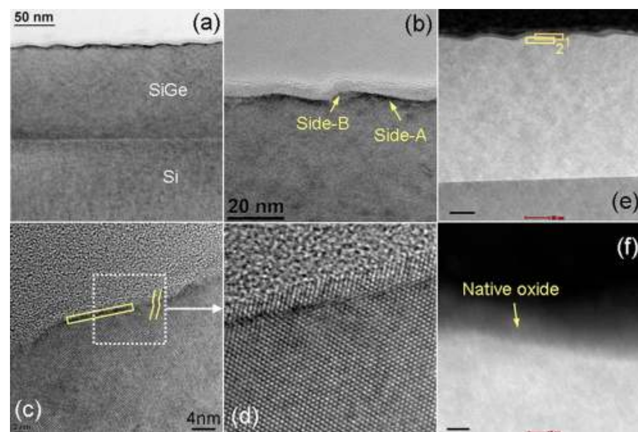

FIG. 2. (Color online) Low magnification bright-field XTEM images [(a) and (b)] and high-resolution XTEM image (c) of the optimized sample. The dashed box in (c) is zoomed in (d). The dislocations and missing atoms in (c) are marked by zigzag lines and by a box, respectively. The locations at which the EDS measurements were performed are indicated by boxes with numbers "1" and "2" in the HAADF-STEM image (e); high-resolution HAADF-STEM image in Side-A (f). Scale bars in [(e) and (f)] are 20 and 2 nm, respectively.

Si. Since the Si and Ge atoms are distributed in the $Si_{0.8}Ge_{0.2}$ layer, the average Z value in this layer would be higher than that of Si alone, and therefore gives different contrast [see Fig. 2(e)]. The high-resolution HAADF-STEM image [Fig. 2(f)] depicts the crystalline nature of the ion beam sputtered SiGe layer. Since the Ge and Si atoms are not distinguishable [Fig. 2(f)], we performed EDS measurements in Side-A at two different areas "1" and "2" (indicated by boxes) in Fig. 2(e). Detailed analyses suggest that the atomic percentages of Si, Ge and O in area-1 and area-2 are of 71%, 19%, and 10% and 75%, 16%, and 9%, respectively, within 10% fluctuation. Clearly, the ~2 nm thick amorphous surface layer [Figs. 2(b) and 2(f)] is the native oxide of the SiGe layers. Prior results revealed[15] that the oxidation of the surface SiGe atoms increases with increasing Ge content. Since the formation enthalpy (ΔG_f) of GeO, GeO_2, and SiO_2 are of −237.2, −521.4, and −856.3 kJ/mol, respectively,[16] it seems that SiO_x will dominate over GeO_x in the native oxide. Moreover, the observed increase in Ge percentage in area-1 [see Fig. 2(e)] is possibly due to an increase in Ge concentration at the surface SiGe layers, in agreement with our μ-Raman results, which will be addressed in the following. Note that the ion erosion process is a surface phenomenon where the atoms are sputtered away from the topmost layers. Therefore, it is very likely that the stoichiometry at the surface will differ from that in the bulk due to the preferential sputtering yields[11] of the alloy components.

In order to evaluate the ion beam induced compositional variation in the SiGe layers we carry out μ-Raman and PL measurements. For instance, Fig. 3 shows the μ-Raman spectra of the virgin sample (SV), S69 and S50. Each spectrum exhibits several weak features besides the Si longitudinal optical (LO)-peak from the Si substrate at ~520.2 cm^{-1} (Ref. 17–19). For clarity, we separate the total range in two zones: 260–470 cm^{-1} (left inset) and 480–535 cm^{-1} (right inset). Three distinct features peaking at ~291.3, 407.6, and 436.5 cm^{-1} in SV are attributed to Ge–Ge, Si–Ge and the

[This article is copyrighted as indicated in the article. Reuse of AIP content is subject to the terms at: http://scitation.aip.org/termsconditions. Downloaded to] IP: 142.104.240.194 On: Tue, 16 Dec 2014 15:53:14

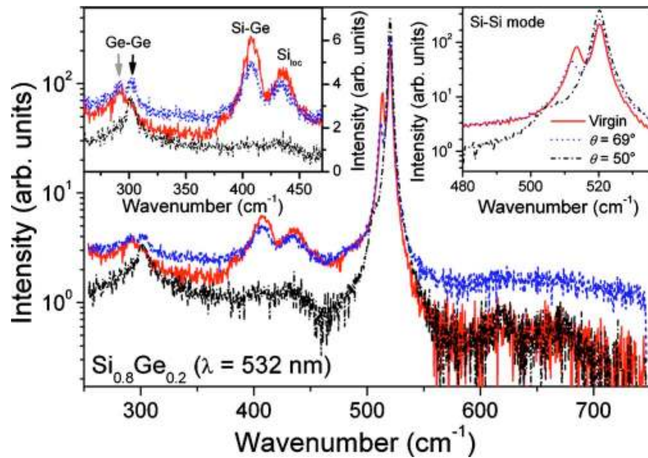

FIG. 3. (Color online) The μ-Raman spectra of the virgin SiGe/Si heterostructure (solid curve), and the ion eroded samples with an incidence angle of 69° (dashed curve) and 50° (dashed-dotted curve). The Ge–Ge, Si–Ge, and Si_{loc} modes (left inset) and the Si–Si modes (right inset) in the range of 260–470 and 480–535 cm^{-1}, respectively, are shown separately for clarity. The Ge–Ge mode (~291.3 cm^{-1}) of the SiGe layer is indicated by downward arrow in light gray (↓), while the first-order Ge–Ge mode of bulk Ge (301.3 cm^{-1}) is marked by downward arrow in black (↓).

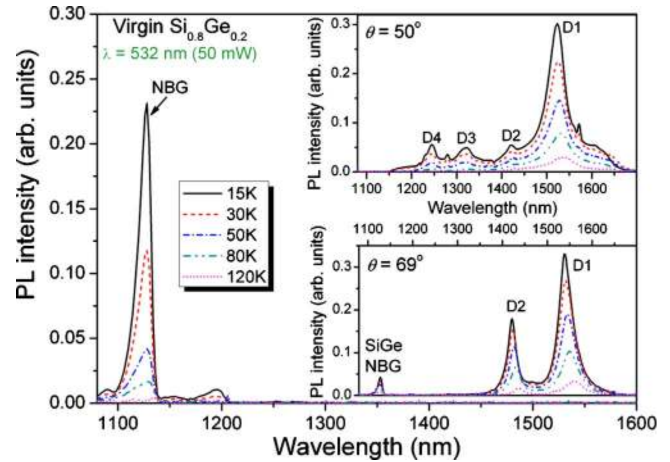

FIG. 4. (Color online) The measurement temperature dependent PL spectra of the virgin SiGe/Si heterostructure (main frame), and the ion eroded samples with an incidence angle of 69° (lower inset) and 50° (upper inset).

localized Si–Si modes of the SiGe layers, respectively.[17–19] The localized Si-Si mode (Si_{loc}) appears due to the reduction of the SiGe alloy's local symmetry by random introduction of Ge atoms in the Si network.[18,19] The 513.6 cm^{-1} peak is assigned to the nearest neighbor Si–Si atomic vibrations in the SiGe layers[20] where the peak position depends not only on the alloy composition but also on biaxial strain ε_{xx}.[19,20] Since SV consists of $Si_{0.8}Ge_{0.2}$ layers, one can calculate a peak position of ~506.6 cm^{-1} in the relaxed $Si_{0.8}Ge_{0.2}$ layers (see Ref. 20 for details). In fact, ε_{xx} can be estimated using an expression:[19] $\Delta\omega_{Si}=(\omega_{Si-Si}-\omega^0_{Si-Si})(cm^{-1})=b_{Si}\varepsilon_{xx}$ where the ω_{Si-Si} and ω^0_{Si-Si} denote the frequencies of the Si–Si mode in strained and relaxed SiGe layers; b_{Si} corresponds to phonon strain-shift coefficient.[17,20] Indeed, the positive $\Delta\omega_{Si}$ confirms compressive strain in the SiGe layers. Using $b_{Si}=-850$ for the Si–Si mode for $x=0.2$,[19] ε_{xx} is calculated to be $\sim 8.5\times 10^{-3}$.

The 513.6 cm^{-1} peak is shifted to 511.9 cm^{-1} in S69 (right inset). However, no marked peak shifting is observed for the Si–Ge mode (left inset). Close inspection reveals that the intensities of the 291.3, 407.6, and 436.5 cm^{-1} peaks are reduced. Another peak is observed at ~301.3 cm^{-1}, which is lying close to the first-order Ge-Ge mode of bulk Ge and the $2TA(X)$ overtone of Si.[17]

Taking into account the preferential sputtering of Si,[11] Ge will enrich at the surface of the SiGe layers. When sputtering reaches the SiGe/Si interface the surplus Ge will accumulate at the surface. In such a situation, the heavy Ge atoms appear to migrate locally to form scattered Ge islands [Fig. 1(b)]. The aforementioned statement is also consistent with μ-Raman results (Fig. 3) where the 301.3 cm^{-1} peak evolves gradually at the expense of the 291.3 and 407.6 cm^{-1} peak intensities by changing the sputtering angle from 69° to 50° from the surface normal. As expected, the negligible change in the Si–Ge peak position in S69 cannot explain the compositional variation in SiGe layers,[20] while the shift in the Si–Si mode from 513.6 cm^{-1} (SV) to 511.9 cm^{-1} (S69) indicates the decrease in strain in the SiGe layers. Indeed, from the absence of the Ge–Ge (291.3 cm^{-1}) and Si–Ge (407.6 cm^{-1}) modes in S50 we can conclude that the SiGe layer thickness is reduced drastically, which is corroborated with the suppression of the Si_{loc} peak intensity (left inset) due to decrease in the localized Si–Si optic phonons in Ge neighborhood. Moreover, the systematic increase in the 520.2 cm^{-1} peak intensity in a sequence of SV, S69, and S50 reveals increasing exposure to the Si substrate due to the decrease in the SiGe layer thickness. Since the Si substrate is covered by ~130 nm thick SiGe layer in S69 [see Fig. 2(a)], we can discard the influence of the $2TA(X)$ overtone of the Si bulk behind the origin of the 301.3 cm^{-1} peak (Fig. 3). Hence, we conclude that this peak is mainly associated with the surface Ge layers[17] of S69, in agreement with our XTEM studies. The increase in the 301.3 cm^{-1} peak intensity in S50 can also be justified in terms of the increase of the Ge–Ge vibrational modes in Ge islands [see Fig. 1(b)].

We also follow the PL properties of the same set of samples by varying the measurement temperature (T) in the range of 15–295 K. Since no PL is detected at high T, we display only the PL spectra of SV (main frame), S50 (upper inset) and S69 (lower inset) up to 120 K (Fig. 4). As discerned (main frame), the PL intensity increases with decreasing T by suppressing the impact of thermal phonons. The strong asymmetric peak at ~1128 nm (1.09 eV) and the adjacent weak peaks at ~1089 nm (1.13 eV), 1154 nm (1.07 eV), and 1196 nm (1.03 eV) can be assigned to the NBG PL signals from the SiGe epilayer where the expression of the X and L bands are: $E^X_g(x)=1.155-0.43x+0.206x^2$ eV and $E^L_g(x)=2.010-1.270x$ eV.[21] Note that the intensity and the linewidth of a specific transition depend on alloy composition.[21,22] Interestingly, the appearance of two extra peaks in S69 at ~1422 nm (0.87 eV) and 1540 nm (0.80 eV), which show a redshift with increasing T, are found relatively stronger than that of the NBG PL of the SiGe layers (lower inset). On the other hand, four main bands peaking at ~1245 nm (0.99 eV), 1322 nm (0.93 eV), 1422 nm (0.87 eV), and 1524 nm (0.81 eV) are noticed in S50 where the

[This article is copyrighted as indicated in the article. Reuse of AIP content is subject to the terms at: http://scitation.aip.org/termsconditions. Downloaded to] IP: 142.104.240.194 On: Tue, 16 Dec 2014 15:53:14

absence of the NBG emission confirms complete sputtering of the SiGe layer, in agreement with our μ-Raman results (Fig. 3). Moreover, a T dependent redshift in the 1524 and 1422 nm bands and a blueshift in the 1322 and 1245 nm bands are the characteristics of the dislocation bands D1-D4.[23] It appears that the surface dislocations [Figs. 2(c) and 2(d)] offer a large number of carriers to recombine radiatively in S69. As the SiGe layer is completely sputtered in S50, it seems that the D1-D4 bands are possibly originating from the ion erosion mediated dislocations in the Si substrate.[24] The origin of the 1280 nm (0.97 eV) PL in S50 is not clear, while the weak 1572 nm (0.79 eV) peak corresponds to the C–O complex.[23]

IV. CONCLUSIONS

In summary, we have demonstrated a transformation of ripples to Ge islands on a strained $Si_{0.8}Ge_{0.2}$ epilayer by varying the incidence angle of 500 eV Ar^+ ions between 69° to 50° from the surface normal for a fixed fluence of 4×10^{17} ions/cm^2. The ripples in 69° sputtered sample are found crystalline covered by a thin oxide layer using high-resolution XTEM and HAADF-STEM, while the EDS and μ-Raman analyses suggest Ge enrichment near the surface. PL investigation reveals two dislocation bands D1 and D2 at ~1540 and 1422 nm, respectively, by suppressing the NBG emission of the $Si_{0.8}Ge_{0.2}$ layers in the rippled sample. However, the NBG PL disappears completely in 50° sputtered sample, instead the dislocation bands D1, D2, D3, and D4 are observed at ~1524, 1422, 1322, and 1245 nm, respectively. We conclude that the near surface dislocations in the rippled sample play the key role for the D1 and D2 bands, whereas the D1-D4 bands in 50° sputtered sample are associated with the ion beam induced dislocations in the Si substrate due to the complete sputtering of the SiGe layer.

ACKNOWLEDGMENTS

Authors would like to acknowledge Dr. B. Tillack from IHP Frankfurt Oder and Dr. M. Voelskow from FZ Dresden-Rossendorf for supplying the samples.

[1] W. L. Chan and E. Chason, J. Appl. Phys. **101**, 121301 (2007).
[2] C. Hofer, C. Teichert, M. Wächter, T. Bobek, K. Lyutovich, and E. Kasper, Superlattices Microstruct. **36**, 281 (2004).
[3] A. Keller, R. Cuerno, S. Facsko, and W. Möller, Phys. Rev. B **79**, 115437 (2009).
[4] S. Facsko, T. Dekorsy, C. Koerdt, C. Trappe, H. Kurz, A. Vogt, and H. Hartnagel, Science **285**, 1551 (1999); T. Bobek, S. Facsko, H. Kurz, T. Dekorsy, M. Xu, and C. Teichert, Phys. Rev. B **68**, 085324 (2003).
[5] E. Chason, T. M. Mayer, B. K. Kellerman, D. T. Mcilroy, and A. J. Howard, Phys. Rev. Lett. **72**, 3040 (1994); S. K. Mohanta, R. K. Soni, S. Tripathy, and S. J. Chua, Appl. Phys. Lett. **88**, 043101 (2006).
[6] M. O. Liedke, B. Liedke, A. Keller, B. Hillebrands, A. Mücklich, S. Facsko, and J. Fassbender, Phys. Rev. B **75**, 220407 (R) (2007).
[7] T. W. H. Oates, A. Keller, S. Noda, and S. Facsko, Appl. Phys. Lett. **93**, 063106 (2008).
[8] R. Moroni, D. Sekiba, F. Buatier de Mongeot, G. Gonella, C. Boragno, L. Mattera, and U. Valbusa, Phys. Rev. Lett. **91**, 167207 (2003).
[9] V. B. Shenoy, W. L. Chan, and E. Chason, Phys. Rev. Lett. **98**, 256101 (2007).
[10] V. Tuboltsev, P. Jalkanen, M. Kolodyazhnaya, and J. Räisänen, Phys. Rev. B **72**, 205434 (2005).
[11] M. Z. Hossain, J. B. Freund, and H. T. Johnson, J. Appl. Phys. **103**, 073508 (2008).
[12] C. Teichert, Phys. Rep. **365**, 335 (2002).
[13] S. Sarkar, B. Van Daele, and W. Vandervorst, Appl. Surf. Sci. **255**, 1368 (2008).
[14] U. Kaiser, D. A. Muller, J. L. Grazul, A. Chuvilin, and M. Kawasaki, Nature Mater. **1**, 102 (2002).
[15] I.-M. Lee and C. G. Takoudis, J. Vac. Sci. Technol. A **15**, 3154 (1997).
[16] *CRC handbook of Chemistry and Physics*, edited by D. R. Lide (CRC, Boca Raton, Florida, 2006).
[17] P. H. Tan, K. Brunner, D. Bougeard, and G. Abstreiter, Phys. Rev. B **68**, 125302 (2003).
[18] M. I. Alonso and K. Winer, Phys. Rev. B **39**, 10056 (1989).
[19] M. Stoehr, D. Aubel, S. Juillaguet, L. Bischoff, L. Kubler, D. Bolmont, F. Hamdani, B. Fraisse, and R. Fourcade, Phys. Rev. B **53**, 6923 (1996).
[20] J. C. Tsang, P. M. Mooney, F. Dacol, and J. O. Chu, J. Appl. Phys. **75**, 8098 (1994).
[21] J. Weber and M. I. Alonso, Phys. Rev. B **40**, 5683 (1989).
[22] G. S. Mitchard and T. C. McGill, Phys. Rev. B **25**, 5351 (1982).
[23] S. Fukatsu, Y. Mera, M. Inoue, K. Maeda, H. Akiyama, and H. Sakaki, Appl. Phys. Lett. **68**, 1889 (1996).
[24] V. Kveder and M. Kittler, Mater. Sci. Forum **590**, 29 (2008).

[This article is copyrighted as indicated in the article. Reuse of AIP content is subject to the terms at: http://scitation.aip.org/termsconditions. Downloaded to] IP: 142.104.240.194 On: Tue, 16 Dec 2014 15:53:14